



## SEISMIC BEHAVIOR AND EVALUATION OF CONCRETE WALLS REINFORCED BY HYBRID HIGH-STRENGTH BARS

L. Zeng <sup>(1)</sup>, Y. Sun <sup>(2)</sup>, T. Takeuchi <sup>(3)</sup>, J. Zhao <sup>(4)</sup>

<sup>(1)</sup> Ph.D. Student, Graduate School of Engineering, Kobe University, zenglx1990@outlook.com

<sup>(2)</sup> Professor, Graduate School of Engineering, Kobe University, sun@person.kobe-u.ac.jp  
China-Japan Resilient and Sustainable Concrete Structures Research Center, Southwest Jiaotong University, China

<sup>(3)</sup> Assistant Professor, Graduate School of Engineering, Kobe University, takeuchi\_t@person.kobe-u.ac.jp

<sup>(4)</sup> Professor, Graduate School of Mechanics and Engineering, Zhengzhou University, zhaoj@zzu.edu.cn  
China-Japan Resilient and Sustainable Concrete Structures Research Center, Southwest Jiaotong University, China

### **Abstract**

It has been well known and experimentally verified that unbonded post-tensioned (UPT) precast concrete walls could provide excellent seismic resilience in terms of self-centering capability. Because the UPT high-strength bars are generally placed near the middle of concrete wall section, they do not provide much resistance to the lateral force induced by earthquake and result in much smaller lateral resistance than that of conventional ductile cast-in-place reinforced concrete walls. In addition, the UPT concrete walls involve difficult construction process and lead to poor cost performance.

To overcome these disadvantages of UPT walls, this paper proposes a new method to enhance the resilience, which is usually expressed in terms of self-centering capability and/or drift-hardening capability, for cast-in-place concrete walls. The new method involves the use of hybrid high-strength bars, including PC strands and/or Carbon Fiber Reinforced Polymer (CFRP) bars as longitudinal rebars placed in shear walls. To verify effectiveness of the new method, three full scale concrete walls were fabricated and tested under reversed cyclic lateral loading while subjected to constant axial load with the type of tensile rebars placed within the edge zones of wall panel as primary experimental variable. One wall was reinforced by eight normal-strength rebars 12 mm in diameter to represent the code-based ductile wall, and two walls were reinforced by eight PC strands of 12.7 mm and CFRP bars of 10 mm, respectively, to give an identical tensile steel ratio for all specimens. All test walls were 2360 mm high by 1280 mm long by 200 mm wide. The shear span ratio was 2.0, while the axial compressive force applied to each wall was 1520 kN to give an axial load ratio of 0.13.

Test results have shown that the residual drift of the wall utilizing PC strands after unloading from 2.5% drift was less than 0.7% as compared with the residual drift of about 1.4% of the code-based ductile wall, which implies that the use of PC strands is very effective to reduce residual deformation. The wall reinforced by CFRP bars also exhibited less residual drift after unloading from 2.5% drift than 0.5%, and indicating that CFRP bar is effective as PC strands in reducing drift deformation and enhancing resilience of concrete walls.

Parallel to the experimental work, an analytical method was presented to evaluate the cyclic behavior of concrete walls reinforced by hybrid high-strength bars, and the theoretical results by the proposed method showed good agreement with the experimental ones.

*Keywords: PC strands; CFRP bars; Residual drift; Residual crack width*



## 1. Introduction

In recent years, we are in a seismic active period. For example, 1379 earthquakes with  $M \geq 5$  and 133 earthquakes with  $M \geq 6$  have taken place around the world in 2019. Frequent aftershocks, high magnitude and long-time earthquakes have made the post-earthquake reconstruction more difficult, and seriously influence people's life. Meanwhile, the downtime and the reconstruction costs have resulted in great burden to the economy. So the aseismic design should turn to resilience from the seismic collapse resistance. In 2009, scholars from America and Japan have pointed out that we should make the "Resilient City" [1] as the goal of earthquake engineering cooperation, which means that the resilient structure becomes one of the mainstreams of seismic research.

Resilient structure includes swaying structure, structure with replaceable members and self-centering structure, and these methods can be combined for the design of structure. The earliest research on the swaying structure can be traced back to Housner's [2] theoretical analysis of the high-level flume that was weakened due to the foundation from damage during the 1960 Chile earthquake. Priestley [3] verified the theory developed by Housner for the free rocking of a rigid block and proposed a response-spectra method for assessing maximum rocking displacements. The structure with replaceable members is a design method that using replaceable structural members to concentrate the plastic deformation and dissipate earthquake energy. The replaceable structural members can be replaced easily, and the function of structure can be restored quickly after the earthquake.

The self-centering structure is derived from the swaying structure. Scholars have conducted a series of experiments, analyzed data and studied the design methods for self-centering structure and shear wall structure in terms of resilient aseismic structure. Kurama [4, 5] verified the self-centering capability of unbonded post-tensioned (UPT) precast concrete walls and presented a new analytical method that using fiber elements. Although the resilient capacity of UPT precast concrete walls are provided by the post-tensioning steel which is not bonded to the concrete, the prestress force may loss during full cyclic loading. Erkmen [6] studied the effects of different design factors on the resilient capacity of UPT precast concrete walls under earthquake loading. These test variables include the arrangement of rebars, the design of end anchor, and axial load ratio. And indicates that even the prestress die out, the self-centering of specimens can be achieved through the proper design. However, the use of unbonded steel bars results in very little energy dissipation and cannot delay or prevent the yielding of post-tensioned tendons in shear walls. Restrepo [7] investigated the seismic performance of self-centering structural walls incorporating energy dissipators. These walls displayed a characteristic "flag-shape" hysteretic response and significantly energy dissipation. Usually the prestressed tendons are placed in the wall panel which is far away from the boundary elements by researchers. This design of shear walls results in a smaller initial stiffness and a larger horizontal displacement than conventional reinforced concrete shear walls under earthquake loading.

Fiber reinforced polymer (FRP) bar is an ideal material with the excellent corrosion resistance and high tensile strength, which can be used as reinforcement bars in building structure. Holden [8] studied the seismic behavior of post-tensioned precast concrete walls which use FRP bars as prestressed tendons and energy dissipating devices. Mohamed's research results [9] showed that the concrete shear wall was fully used of glass fiber reinforced polymer (GFRP) bars as reinforcement bars, and displayed these walls can meet requirements of bearing capacity and drift ratio in different codes. The research team of the authors [10] have studied the use of carbon fiber reinforced polymer (CFRP) bars to replace the steel bars in concrete shear walls and found that the proper replacement ratio and position could improve the bearing capacity and reduce residual deformation.

This paper investigates the effect of hybrid high-strength bars, including PC strands and CFRP bars as longitudinal rebars placed in shear walls without initial prestress. In this study, the PC strands in two walls were placed as longitudinal tensile bars in boundary columns, and one of the walls used CFRP bars as longitudinal bars in the wall panel. In addition, the other shear wall used normal steel bars were fabricated for comparison.



## 2. Experimental test methodology

An experimental research was conducted to investigate the resilient capacity of cast-in-place walls reinforced with hybrid high-strength bars. All test walls had embedded columns, and the size of columns was the same with wall panel.

### 2.1 Construction detail

In this study, three reinforcement concrete walls with the same dimensions were designed to be 2360 mm high, 1280 mm long and 200 mm thick with a loading beam at the top as shown in Fig.1. Three identical geometry specimens with the different variety of vertical bars were tested up to failure under reversed cyclic lateral loading. The experimental variables among three walls were the variety of reinforcement bars in the wall panel and boundary columns, respectively. The name of each test specimen indicated the type of high-strength bars in walls. Specimen RCSW was a traditional reinforcement concrete shear wall. Specimen STSW was reinforced with PC strands in boundary columns. Based on specimen STSW, Specimen CFRP-STSW was reinforced with CFRP bars to replace longitudinal steel bars in wall panel. As one can see from Table 1 and Fig.1 (a~c), each grid in wall panel was comprised of C8 (steel bars, 10 mm in diameter) bars with a spacing of 60 mm in horizontal direction. In order to keep the same vertical reinforcement ratio, the spacing of C10 bars was 115mm (CFRP bars, 10 mm in diameter). Both the reinforcement ratio of vertical and horizontal bars met the requirement of JGJ 3-2010 (larger than 0.25%) [11] and ACI 318 (larger than 0.15% and 0.25%, respectively) [12].

Fig.2 (a~c) displays the reinforcement details of three specimens for different design with cross section. The tensile tendons in boundary columns of specimen RCSW were consisted of eight C12 (steel bars, 12 mm in diameter) rebars, and eight PC strands (1x7, 12.7 mm in diameter) were placed in boundary columns of specimen STSW and specimen CFRP-STSW, respectively. The boundary columns of all specimens had rectangular stirrups, were C6 (steel bars, 6 mm in diameter) bars with a spacing of 70 mm. Table 1 summarizes the design parameters of three specimens, include concrete strength, the ratio of axial load and shear span, reinforcement details. The axial load force was applied to each specimen was 1520 kN, and the actual concrete strength and axial load ratio were 45.9 MPa and 0.13, respectively.

Table 1 – Test details of all specimens

Specimens	Axial load ratio	Shear span ratio	Wall panel		Boundary column	
			$p_{wh}$ (%)	$p_{wv}$ (%)	Grade	$p_t$ (%)
RCSW	0.13	2	0.71	0.71	HRB400	0.37
STSW	0.13	2	0.71	0.71	PC12.7	0.33
CFRP-STSW	0.13	2	0.71	0.71	PC12.7	0.33

Note:  $p_{wh}$ - the steel ratio of horizontal reinforcement bars in web panel;  $p_{wv}$ - the steel ratio of vertical reinforcement bars in web panel;  $p_t$ - the steel ratio of tensile rebars.

To avoid the phenomenon of pre-tensioned and premature slip of PC strands which affects experimental results, both top and base ends of each PC strand in specimen STSW and specimen CFRP-STSW were anchored to 10 mm-thick steel plates as shown in Fig.2 (d~e) and Fig.3. Fig.2 (f) displays the shape of horizontal bars and stirrups.

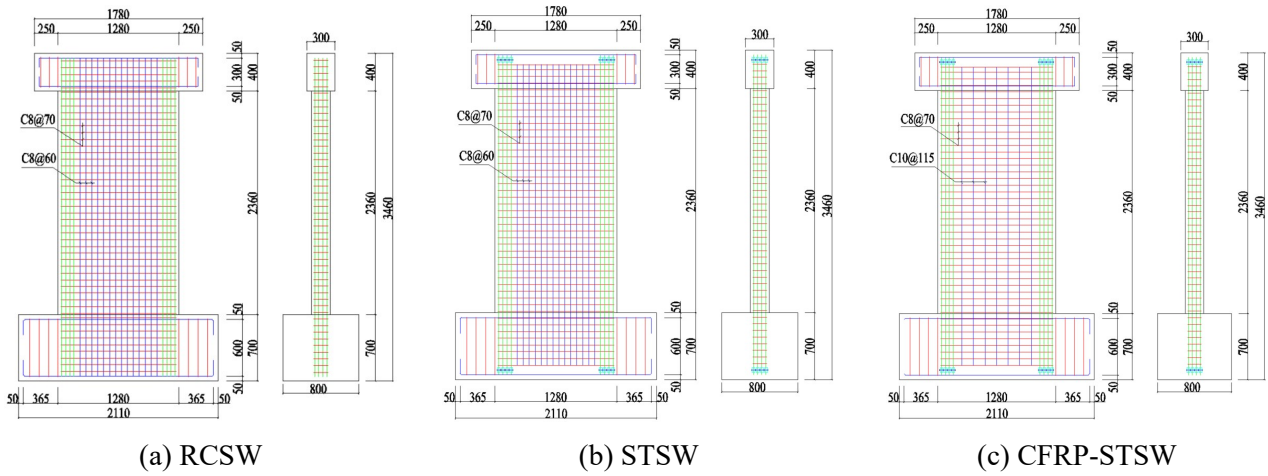
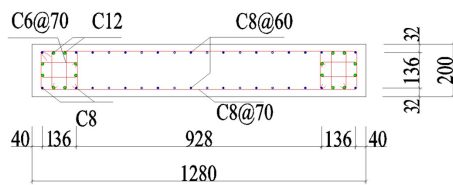
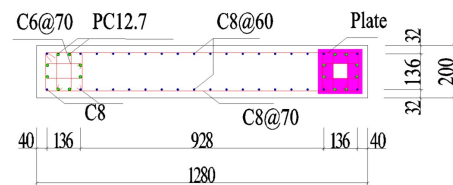


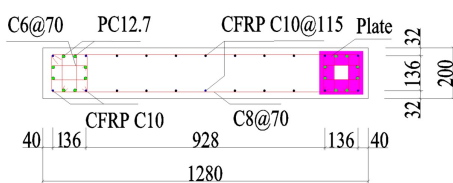
Fig. 1 – Reinforcement details and dimensions of specimens (in mm, elevation)



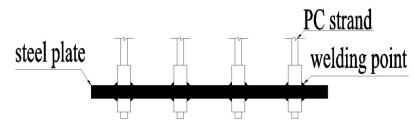
(a) RCSW



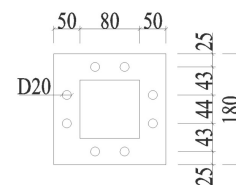
(b) STSW



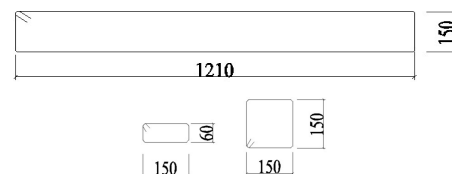
(c) CFRP-STSW



(d) Details of anchorage



(e) End plate



(f) Horizontal bars and stirrups

Fig. 2 – Reinforcement details of specimens (in mm, cross section)



Fig. 3 – Anchorage setup for PC strands



## 2.2 Material properties

All specimens were fabricated with ready-mixed concrete and the concrete cubes (150mm x 150 mm x 150 mm) strength ( $f_{cu}$ ) was 55.3 MPa. The concrete cylinder (200mm high by 100mm diameter) strength ( $f_c'$ ) was 45.9 MPa. Table 2 displays the properties of concrete. The steel bars (HRB 400 MPa, 6~12 mm in diameter), PC strands and CFRP bars were placed as horizontal bars and vertical bars in specimens. Test values of all reinforcement as shown in Table 3.

Table 2 – Mechanical properties of concrete

$f_{cu}$ (MPa)	$f_c'$ (MPa)	$f_t$ (MPa)	$E$ (MPa)
55.3	45.9	3.4	$3.54 \times 10^4$

Note:  $f_{cu}$ - cubic compressive strength of concrete;  $f_c'$  - concrete cylinder strength;  $f_t$ - split-tensile strength;  $E$ - elastic modulus in compression.

Table 3 – Mechanical properties of steel bars, PC strands and CFRP bars

Bars	Diameter (mm)	Yield strength (MPa)	Ultimate strength (MPa)	Yield strain (%)	Elongation (%)	Modulus (MPa)
C6	6	490	662	0.22	35.0	$2.19 \times 10^5$
C8	8	544	682	0.27	23.7	$2.03 \times 10^5$
C12	12	473	627	0.23	8.5	$2.06 \times 10^5$
PC strand	12.7	1753	1890	0.89	5.5	$1.97 \times 10^5$
CFRP bar	10	-	1102	-	-	$1.02 \times 10^5$

Note: The yield strength of PC strands- 0.2 % offset yield strength.



Fig. 4 – Loading apparatus

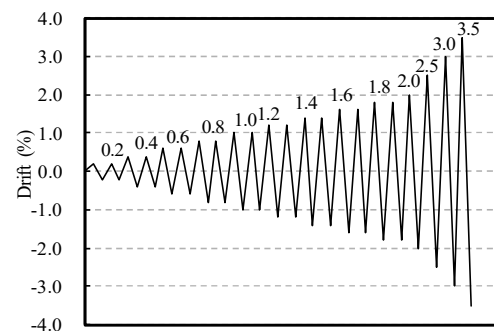


Fig. 5 – Loading system

## 2.3 Test method

Three specimens were constructed and tested under reversed cyclic loading in the lab of structural engineering. The photograph of specimen and experiment setups as shown in Fig.4. To eliminate vertical and horizontal displacement, the foundation of specimen was fixed to the laboratory floor and restrained by two hydraulic jacks and two steel girders. An axial load of 1520 kN was applied by two hydraulic jacks (maximum capacity: 2000 kN) situated at the top of each specimen to simulate gravity loadings. The reversed-cyclic loading was provided by the actuator (maximum capacity: 2500 kN), and the loading height was 2560 mm from the foundation beam.



The reversed-cyclic loading was controlled by the drift as shown in Fig.5. Each drift level was applied with two cycles before the drift less than or equal to 2.0%, and subsequent drift target was applied with one cycle at the drift of 2.5%, 3.0%, and 3.5%, respectively. Arrangements of displacement transducers for measuring the horizontal (DH) and vertical (DV) displacement as illustrated in Fig.6. Fig.7 displays the layout of strain gauges.

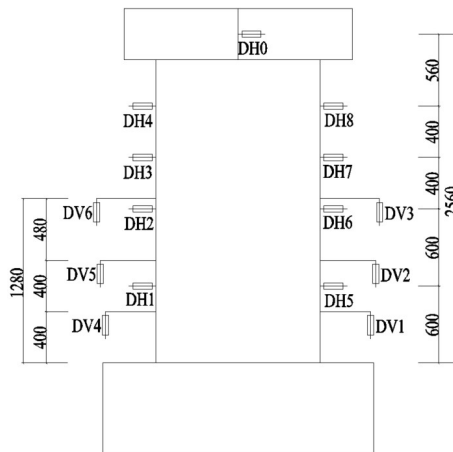


Fig. 6 – Arrangements of displacement transducers

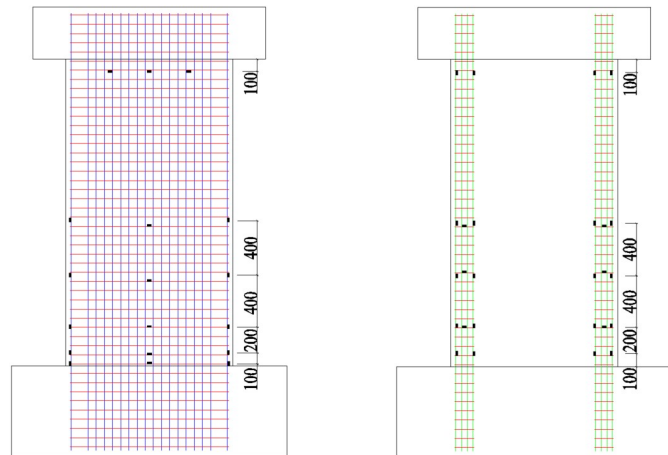


Fig. 7 – Arrangements of strain gauges

### 3. Results and discussion

#### 3.1 Failure modes

Table.4 summarizes experimental results of the ultimate flexure strength and drift ratio capacity of three specimens. And the calculated flexural ( $V_{fu,ACI}$  and  $V_{fu,AIJ}$ ) bearing capacity and shear ( $V_{su,ACI}$  and  $V_{su,AIJ}$ ) bearing capacity were based on code equations of ACI [12] and AIJ [13].

Table 4 – Experimental results and calculated results of the test walls

Specimens	Measured results		Estimated results				Failure modes
	$V_{exp}$ (kN)	$R_{exp}$ (%)	$V_{fu,ACI}$ (kN)	$V_{fu,AIJ}$ (kN)	$V_{su,ACI}$ (kN)	$V_{su,AIJ}$ (kN)	
RCSW	697	0.97	667	720	1277	985	Flexure
STSW	973	2.47	759	1062	748	853	Flexure
CFRP-STSW	944	1.95	1017	1186	1225	972	Flexure

Note:  $V_{exp}$ - the average value of measured maximum lateral force;  $R_{exp}$ - the drift ratio at  $V_{exp}$ .

The crack patterns and failure modes of three specimens were measured at the final damage state as shown in Fig.8 (a~c). All specimens display a flexure failure mode and a similar failure process. With the increases of lateral drift, concrete cover spalling, crushing and then longitudinal reinforcement bars deformed at the boundary columns, and then fell to failure finally. The concrete spalling of specimen RCSW was more serious than specimen STSW and specimen CFRP-STSW. The conclusion can be shown that setting PC strands in boundary columns can improve the concrete damage of specimen. Compared with specimen STSW, the damage of specimen CFRP-STSW was propagated extensive diagonal cracks, and these cracks distributed



along the whole height of specimen. The reason is that CFRP bar is a kind of linear-elastic material with high bond-slip strength which compared with ordinary steel bars. The damage patterns of specimens reinforced with PC strands were similar, the reason of bearing capacity degradation was the crushing of PC strands at the boundary column toes.

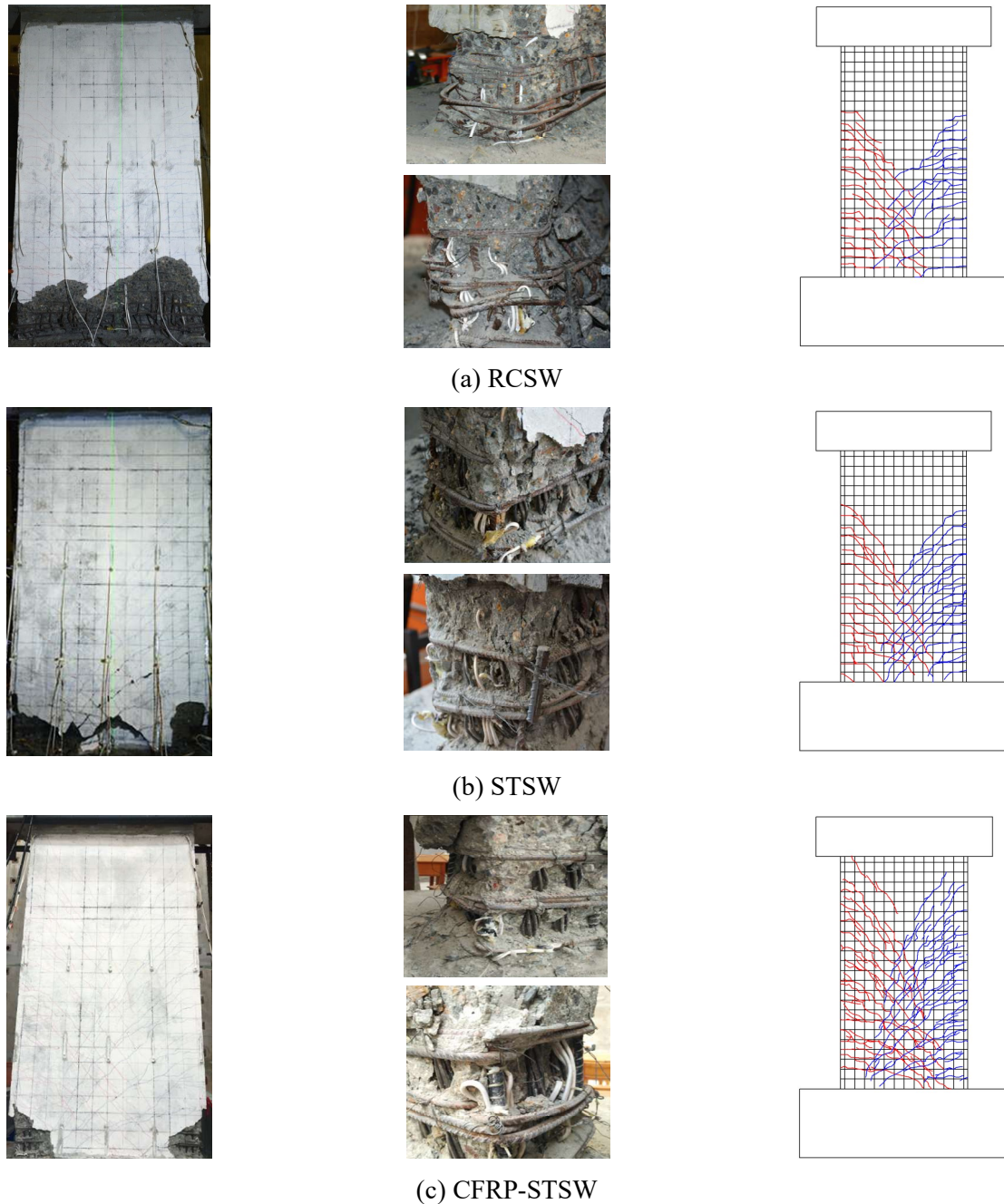


Fig. 8 – Crack patterns and failure modes

Fig.9 displays the characteristic curves of maximum crack width and residual crack width were measured at different drift levels. According to Fig.9 (a), the maximum crack width of specimen RCSW had inclined cracks at the drift ratio of 0.17%, and increased rapidly with the subsequent drift levels. Eventually a



crack which reached to 3 mm at the drift ratio of 2.5 %. By contrast, the maximum crack width of specimen STSW and specimen CFRP-STSW remained less than 1.2 mm until 2.5 % drift, which means the crack width reduced by 60 % and 70 %, respectively. Compared with the specimen STSW, the main difference was that the specimen CFRP-STSW had CFRP bars in wall panel and the hybrid high-strength bars could further reduce the maximum crack width. As shown in Fig.9 (b), the specimen RCSW had residual crack width of 2.2 mm at the drift ratio of 2.5 %, while the values of specimen STSW and specimen CFRP-STSW were only 0.17 mm and 0.26 mm, respectively. Therefore, the phenomenon revealed that placing PC strands with no prestressed in boundary columns can also effectively improve the residual crack width.

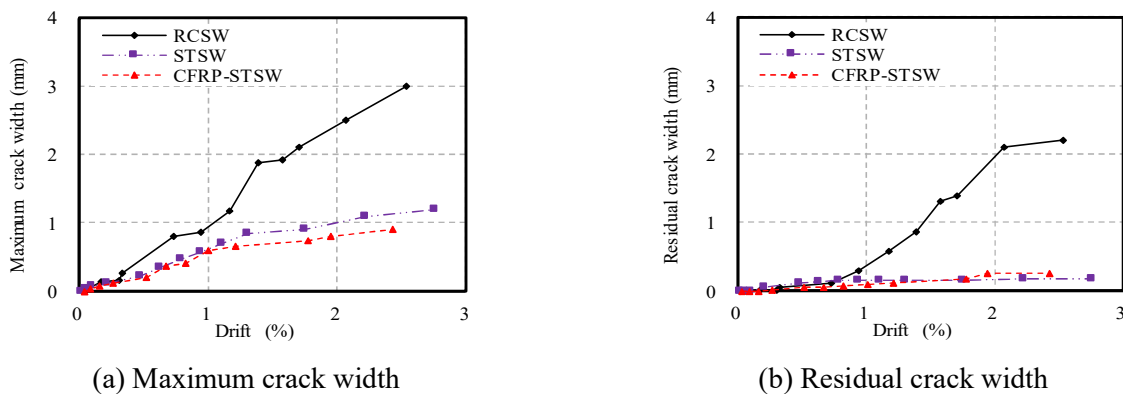


Fig. 9 – Maximum crack width and residual crack width

### 3.2 Lateral load-top displacement response

The lateral load-displacement hysteretic curves of each specimen as shown in Fig.10. The curve shape of specimen RCSW was plumper than the other specimens at the same drift level, and exhibited typical ductile characteristics of the conventional reinforcement concrete wall. And specimens which placed PC strands in boundary columns displayed more pinched hysteretic loops than specimen RCSW. The reason is that the energy dissipation mainly through the yield of vertical bars at the plastic hinge region in monolithic shear walls, and the use of PC strands in boundary columns did not significantly yield at the plastic hinge region. By comparing the hysteretic curves of three specimens, the drift-hardening ability of specimen STSW and specimen CFRP-STSW were greater than specimen RCSW. Besides the shape and size of curves show that these two specimens display a better self-centering ability.

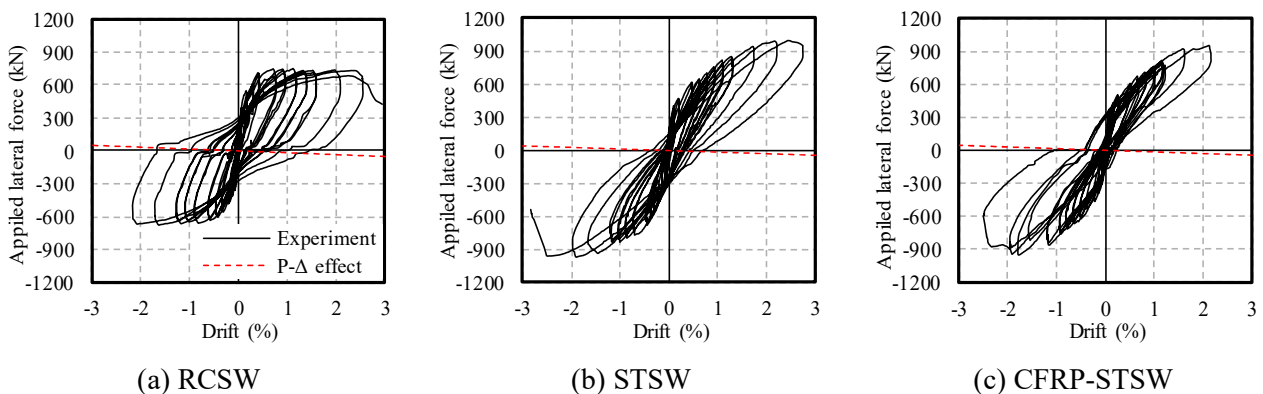


Fig. 10 – Hysteretic curves



Fig.11 (a~c) displays the comparison of envelop curves. Specimen RCSW, specimen STSW and specimen CFRP-STSW achieved their lateral peak loads with 697 kN, 973 kN and 944 kN at the corresponding drift levels of 0.97 %, 2.47 %, 1.95 %, respectively. Specimen STSW had the largest drift capacity and lateral force imply that the lateral resistance continuously increased by using PC strands in boundary columns, and the degradation caused by the P- $\Delta$  effect and the concrete cover spalling can be sufficiently compensated. However, the improvement of the bearing capacity was not significantly by placing CFRP bars in wall panel, and the envelope curves of two specimens which have PC strands were similar as shown in Fig.11 (b). Compared with specimen RCSW, the lateral capacities of specimens reinforced with PC strands and CFRP bars were on ascending stage and with the rising of drift ratio up to the peak load.

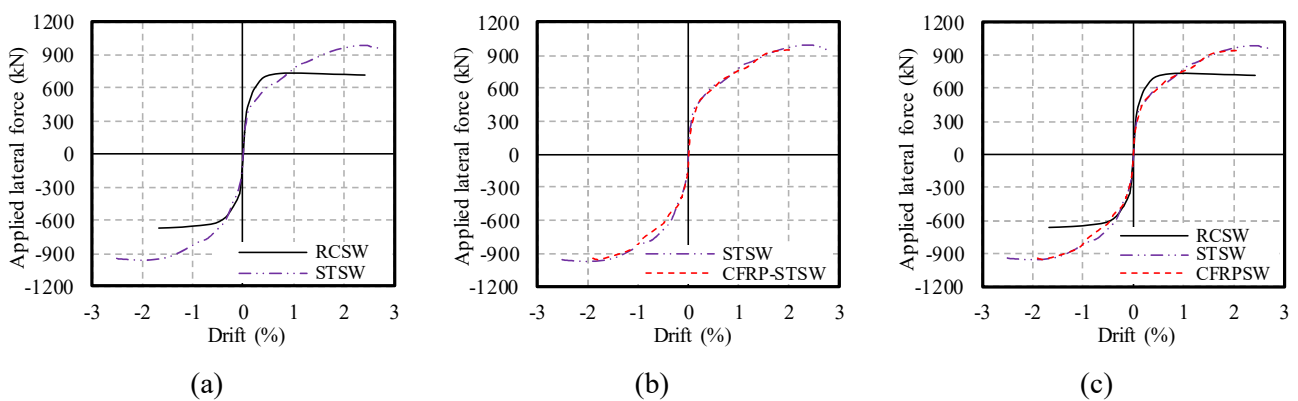


Fig. 11 – Comparison of measured envelop curves

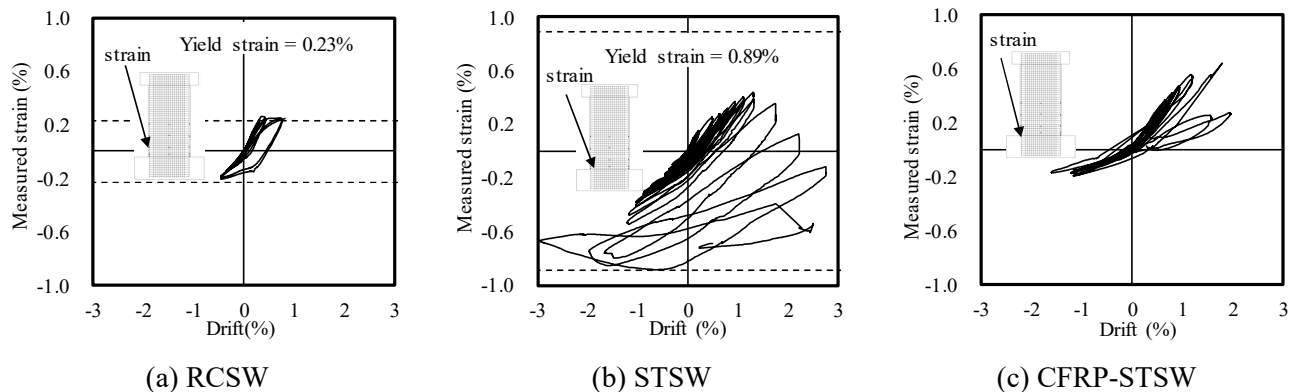


Fig. 12 – Strain of C12 rebar, PC strand and CFRP bar

Note: The horizontal dashed represent the respective yield strains of C12 rebar and PC strand; the arrow shaped line points to the position of the strain gage.

### 3.3 Strain analysis of rebars

The steel strains-drift curves of C12 rebar, PC strand and CFRP bar in boundary columns as shown in Fig.12. Fig.12 (a) shows that the longitudinal reinforcing bar was yielded at drifts between 0.5% and 0.9%. Fig.12 (b) shows the steel strain of PC strand in specimen STSW began to decrease from tension to compression at the drift ratio of 1.5% and began to yield at the drift ratio of 2.5%, then the PC strand began untwisting like



Fig.8 (b). Due to the use of hybrid high-strength bars in specimen CFRP-STSW, the CFPR bar not yielded until the drift ratio of 2.0%, which was higher than RCSW as shown in Fig.12 (c).

### 3.4 Residual drift

The comparison of the measured residual drifts as shown in Fig.13. Specimen RCSW experiences a rapidly increasing residual drift when the peak drift well in excess 1.0%. During the whole experiment, the maximum residual drift of specimen STSW was 0.7% and the corresponding peak drift was 2.7%, which meant the deformation recovered 74% after unloading. Despite specimen CFRP-STSW had the minimum residual drift with the steady increase of lateral drift from 0.2% to 1.7 %, the trend curve was similar as specimen STSW, and its residual drift rose up to 0.40%, 0.45% and 0.56% at lateral drifts of 1.7%, 2.0% and 2.5%, respectively. Based upon the above analysis, it could be concluded that PC strands and CFRP bars can provide excellent resilient capacity compared with conventional steel bars.

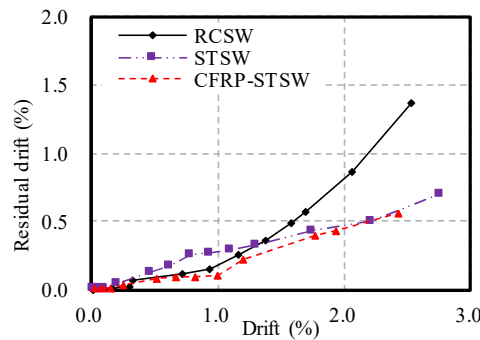


Fig. 13 – Residual drift

## 4. Parametric analysis

### 4.1 Analytical method

To simulate the complete cyclic behavior of specimens reinforced with hybrid high-strength bars, an analysis method was presented which take account of the slippage effect [14] of PC strands, then the basic assumptions are made as follows: 1) concrete does not resist tensile stress; 2) the concrete plane remains plane after bending; 3) lateral displacement of member will concentrate in plastic hinge region of 0.5D (where D is the section length of test wall); 4) strain and stress of rebars are uniformly distributed within the plastic hinge region; 5) the constitutive laws of the concrete are known from reference [15]; 6) the bond-slip relationship of the PC strand follows the method developed by Funato [16]. The member's dissection of analysis model as shown in Fig.14.

### 4.2 Analytical results

Fig.15 displays the comparison of experimental and analytical results. During all analysis steps, the hysteresis curves of experimental and analytical results for specimen RCSW can be ideally matched without considering the slippage effect of C12 steel bars as shown in Fig.15 (a). The slippage effect of PC strands was considered for specimen STSW and specimen CFRP-STSW. Fig.15 (b) shows that the result can match well before the drift ratio reached 2.0 % of specimen STSW. The analytical result of specimen CFRP-STSW was similar to the experiment result, the bearing capacity increased with the increase of drift ratio as shown in Fig.15 (c). Considering the slippage effect of PC strands, the erro range of peak load between experimental values and analytical values were less than 10%.

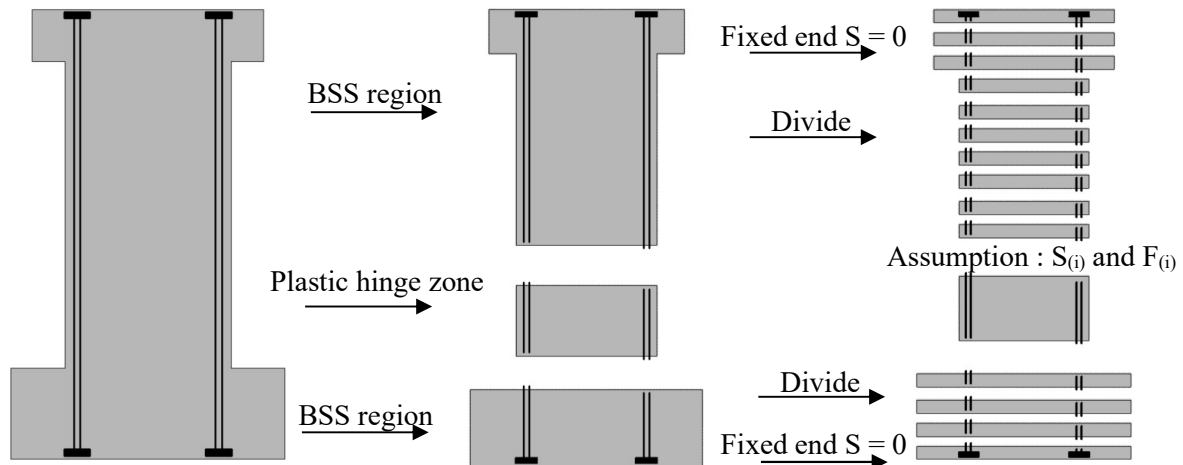


Fig. 14 – Member's dissection of analysis model

Note: BSS- bond-slip spring;  $S_{(i)}$ - the slip in the  $i$ -th segment facing to the hinge region;  $F_{(i)}$ - the rebar stress in the  $i$ -th segment facing to the hinge region.

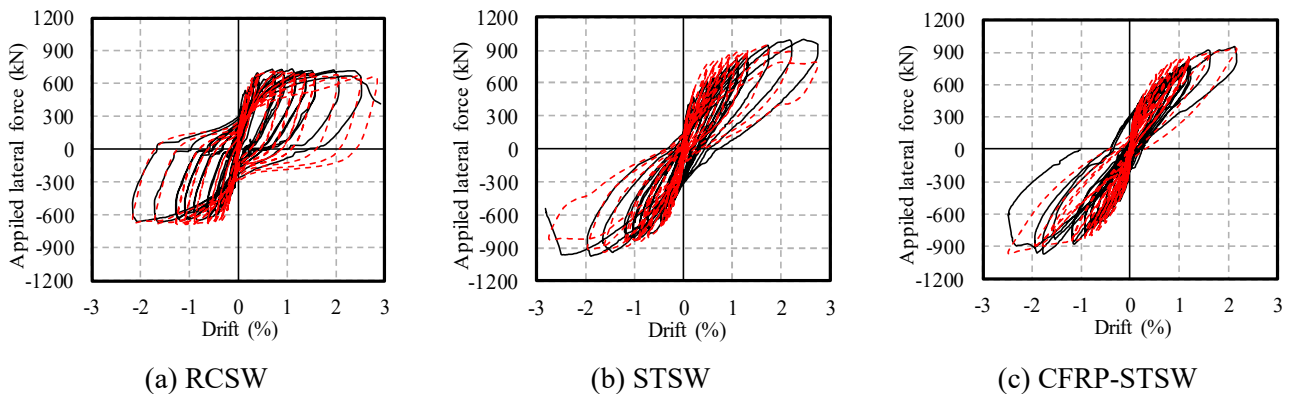


Fig. 15 – Comparison of analytical and experimental results

## 5. Conclusions

This paper aimed to verify the effectiveness of seismic behavior that using hybrid high-strength bars as longitudinal steels placed in shear walls. Three full scale concrete walls were fabricated and tested under reversed cyclic loading. The conclusions of the experiment can be summarized as follows:

1) Using PC strands as vertical bars to replace C12 rebars which in boundary columns could increase the peak lateral resistance by 40%, and reduce the width of residual drift and drift crack by 46% and 60%, respectively. And the shear wall reinforced with hybrid high-strength bars could exhibit excellent drift-hardening capability and the lateral resistance was on ascending stage with the rising of drift ratio up to peak load.

2) The crack processes of all specimens were similar and dominated by flexure failure. The use of PC strands and CFRP bars could improve concrete spalling and provide excellent self-centering capacity compared with conventional steel bars.

3) The calculation method in ACI code and AIJ code were able to accurately predict the ultimate flexural strength of shear walls with hybrid high-strength bars.



4) The hysteresis curves of experimental and theoretical results were relatively satisfactory, and indicate that reliability and accuracy of the analytical method. The analytical method takes into account of slippage effect of PC strands and effectively evaluate the cyclic behavior of the proposed hybrid high-strength concrete shear walls.

## 6. Acknowledgements

The experimental work described in this paper was financially supported by the National Key R&D Program of China (2016YFE0125600) and Program for Innovative Research Team of Education Ministry of China (IRT\_16R67). The first author would to acknowledge the China Scholarship Council (201707040123), Japanese Government (MEXT) Scholarship Program and Zhengzhou University for supporting his overseas study scholarship.

## 7. References

- [1] Report of the seventh joint planning meeting of NEES/E-Defense collaborative research on earthquake engineering. *Report PEER 2010/109*, Pacific Earthquake Engineering Research, Berkeley, USA.
- [2] Housner GW (1963): The behavior of inverted pendulum structure during earthquakes. *Bulletin of the Seismological Society of America*, **53** (2), 403-417.
- [3] Priestley MJN, Evison RJ, Carr AJ (1978): Seismic response of structures free to rock on their foundations. *Bulletin of the New Zealand National Society for Earthquake Engineering*, **11** (3), 141-150.
- [4] Kurama Y, Pessiki S, Sause R, Lu LW (1999): Seismic behavior and design of unbonded posttensioned precast concrete walls. *Precast/Prestressed Concrete Institute Journal*, **38** (3), 72-93.
- [5] Kurama Y, Sause R, Pessiki S, Lu LW (1999): Lateral load behavior and seismic design of unbonded post-tensioned precast concrete walls. *American Concrete Institute Journal*, **96** (4), 622-632.
- [6] Erkmén B, Schultz A (2009): Self-centering behavior of unbonded, post-tensioned precast concrete shear walls. *Journal of Earthquake Engineering*, **13** (7), 1047-1064.
- [7] Restrepo JI, Rahman A (2007): Seismic performance of self-centering structural walls incorporating energy dissipaters. *Journal of Structural Engineering*, **133** (11), 1560-1570.
- [8] Holden T, Restrepo J, Mander JB (2003): Seismic Performance of Precast Reinforced and Prestressed Concrete Walls. *Journal of Structural Engineering*, **129** (3), 286-296.
- [9] Mohamed N, Farghaly AS, Benmokrane B, Neale KW (2009): Experimental Investigation of Concrete Shear Walls Reinforced with Glass Fiber-Reinforced Bars under Lateral Cyclic Loading. *Journal of Composites for Construction*, **18** (3), A4014001.
- [10] Zhao Q, Zhao J, Dang JT, Chen JW, Shen FQ (2019): Experimental investigation of shear walls using carbon fiber reinforced polymer bars under cyclic lateral loading. *Engineering Structures*, **191**, 82-91.
- [11] Ministry of Housing and Urban-Rural Development of the PRC. *Code for seismic design of buildings (GB50011-2010)*.
- [12] American Concrete Institute (2014): *Building code requirements for structural concrete (ACI318-14)*.
- [13] Architectural Institute of Japan (2010): *Standard for structural calculation of reinforced concrete structural (AIJ2010)*.
- [14] Sargayan G, Cai G, Takeuchi T, Sun Y (2017): Seismic behavior and assessment of drift-hardening concrete columns. *16<sup>th</sup> World Conference on Earthquake Engineering*, Santiago, Chile.
- [15] Sun Y, Sakino K, Yoshioka T (1996): Flexural behavior high-strength RC columns confined by rectilinear reinforcement. *Journal of Structural and Construction Engineering*, **61** (486), 95-106.
- [16] Funato Y, Sun Y, Takeuchi T, Cai G (2012): Modeling and application of bond characteristic of high-strength reinforcing bar with spiral grooves. *Proceedings of the Japan Concrete Institute*, **34** (2), 157-162 (in Japanese).